Spectroscopic Analysis of Diamide Ligands as Potential Anion Receptors by using Combination of ¹H NMR and DFT Studies

Nur Shuhaila Haryani Abd Haris¹, Suhaila Sapari², Fazira Ilyana Abdul Razak² and Maisara Abdul Kadir¹,3*

¹Faculty of Science and Marine Environment, Universiti Malaysia Terengganu, 21030 Kuala Nerus, Terengganu ²Department of Chemistry, Faculty of Science, Universiti Teknologi Malaysia, 81310, UTM Johor Bahru, Johor, Malaysia

³Advanced Nano Materials (ANoMa) Research Group, Faculty of Science and Marine Environment, Universiti Malaysia Terengganu, 21030 Kuala Nerus, Terengganu, Malaysia *Corresponding author (e-mail: maisara@umt.edu.my)

Developing anion receptors has garnered significant attention and enthusiasm among researchers owing to the pivotal role of anions in various processes and applications. The development of receptors to remove harmful pollutants is crucial because anion abundance can harm ecosystems. Therefore, in this study five diamide compounds namely 1,2-bis[N,N'-6-(4-pyridylmethylamido) pyridyl-2-carboxyamido]ethane (L1), 1,2-bis[N,N'-6-(4-pyridylmethylamido)pyridyl-2-carboxy amido|propane (L2), 1,2-bis[N,N'-6-(4-pyridylmethylamido)pyridyl-2-carboxyamido|butane (L3), 1,2-bis[N,N'-6-(4-pyridylmethylamido)pyridyl-2-carboxyamido]pentane (L4) and 1,2-bis [N,N'-6-(4-pyridylmethylamido)pyridyl-2-carboxyamido]hexane (L5) were synthesized to explore the hydrogen bonding interactions with chloride, bromide, nitrate, phosphate and chromate anions. ¹H NMR spectroscopy and Density Functional Theory (DFT) calculations were employed to explore the binding affinities of the ligands. ¹H NMR titrations revealed distinctive shifts in the NH proton signals upon interaction with anions, particularly showing strong hydrogen bonding with chloride and phosphate anions. Titration with nitrate displayed upfield shifts, attributed to the presence of internal charge transfer. DFT calculations demonstrated that the combination of ligands and phosphate anions was the most stable, as indicated by the lowest binding energies. Both 1H NMR and DFT results consistently showed that chloride and phosphate formed the most stable complexes with the ligands, demonstrating their high selectivity for these anions.

Keywords: Amide; anion receptors; titration; hydrogen bonding; DFT studies

Received: April 2025; Accepted: August 2025

Supramolecular chemistry is a developing field that focuses on a discrete number of molecules, where weaker chemical forces, such as electrostatic interactions, hydrogen bonds, and Van der Waals forces, are utilized in molecular assemblies. It has attracted considerable interest owing to its potential applications in anion recognition [1], drug delivery [2], catalysis [3], and cationic receptors [4]. One notable application of supramolecular chemistry is in addressing environmental challenges, such as anion-induced water pollution.

Anions from fertilizer runoff, agricultural waste, and industrial waste have been reported to cause water pollution [5]. Excessive intake of chloride may cause severe damage or poisoning to the living body, such as mutations in genes that encode chloride channel proteins (ClCs), which are closely associated with various genetic disorders, including cystic fibrosis and epilepsy [6]. Excessive nitrate levels in aquatic environments can lead to water eutrophication and soil acidification [7]. Consistent consumption of vegetables containing high nitrate concentrations and

drinking water can pose health risks to humans, including the potential for gastric cancer [8], methemoglobinemia, particularly in infants and children, thyroid disorders [9], spontaneous abortions, and congenital disabilities. Excess phosphate is another factor that leads to eutrophication. Consuming water contaminated with phosphate can pose a significant public health concern due to its potential association with hypertension, mineral and bone disorders, vitamin D deficiency [10], tissue calcification, cardiovascular complications, and crystal deposition disease [11].

Anion receptors are designed to recognize, respond to, and sense negatively charged species [12]. Extensive efforts spanning several decades have been dedicated to exploring and identifying receptors capable of recognizing and separating anionic species from other species. As the field has progressed, it is now well established that the inclusion of one or more hydrogen bond donor groups, such as amine, (thio)amide, (thio)urea, pyrrole, or indole groups, is crucial for anion-coordinating receptors or sensors

[13]. Various noncovalent interactions have been used, such as hydrogen bonding [14], anion- π interactions [15], van der Waals forces, electrostatic interactions, hydrophilic and hydrophobic interactions, and coordination with metal ions [16].

In anion-receptor chemistry, hydrogen bonds are fundamental interactions used to stabilize complexes with negatively charged species (anions). Anion recognition via hydrogen bonding is significant because of its directionality, which is helpful in designing selective hosts for anions with different geometries [17]. Receptors are known to be good hydrogen bond donors, whereas anions are good hydrogen bond acceptors, making them well-suited for hydrogen-bonding interactions [18]. Amide receptors are often constructed because they can utilize hydrogen bonding (-NH group) or a combination of hydrogen bonding and electrostatic interactions. By designing a flexible ligand, its conformation can be adjusted for the reversible inclusion and removal of guest molecules [19]. These ligands can form rotatable single bonds owing to their bond angles and distances, allowing them to adapt to different conformations and capture a wide range of anion sizes.

Thus, this study explores the potential of diamide compounds bearing different spacers to act as anion receptors. Figure 1 shows the structures of the five types of dicarboxamide ligands designed as potential anion receptors. The use of pre-organized amides as pendant arms between spacers enhances ligand flexibility. In addition, adding carbon chains to the spacers allows the study of highly flexible

amide ligands with improved structural adaptability. These aliphatic amine spacers enable free torsion from 0 to 360°, providing a space capable of accommodating anions of various sizes and geometries. This design contains tetradentate binding sites, ensuring sufficient space for large anions to interact with the amide NH groups. Furthermore, donor atoms such as nitrogen and oxygen in amides can chelate metals and form stable complexes. The pyridine groups can increase the number of N-coordination sites by supporting the high-dimensional structures. Overall, hydrogen bonding and electrostatic interactions stabilize these flexible ligands, which can adapt to different coordination environments. This research outlines further investigations combining ¹H NMR and DFT studies to provide a deeper understanding of the hydrogen bonding interactions within the NH amide anion pocket. In this study, the anions selected for binding investigations were chloride (Cl-), bromide (Br-), nitrate (NO₃⁻), phosphate (PO₄³⁻), and chromate (CrO₄²⁻), based on their environmental relevance and differing size, charge, and hydrogen bonding capabilities.

As mentioned in the literature, the presence of the NH group allows for hydrogen bonding interactions with anionic species (NH···O), facilitating the encapsulation of anionic guests within the cavity [10]. As reported [20], there are strong intermolecular hydrogen bond interactions between the receptor at NH amide donors and perchlorate anions NH···O (d=2.183) in the crystal packing. This study anticipates that the interactions between the ligand and anions will occur through the amide (NH) moiety via hydrogen bonding as proposed (Figure 2).

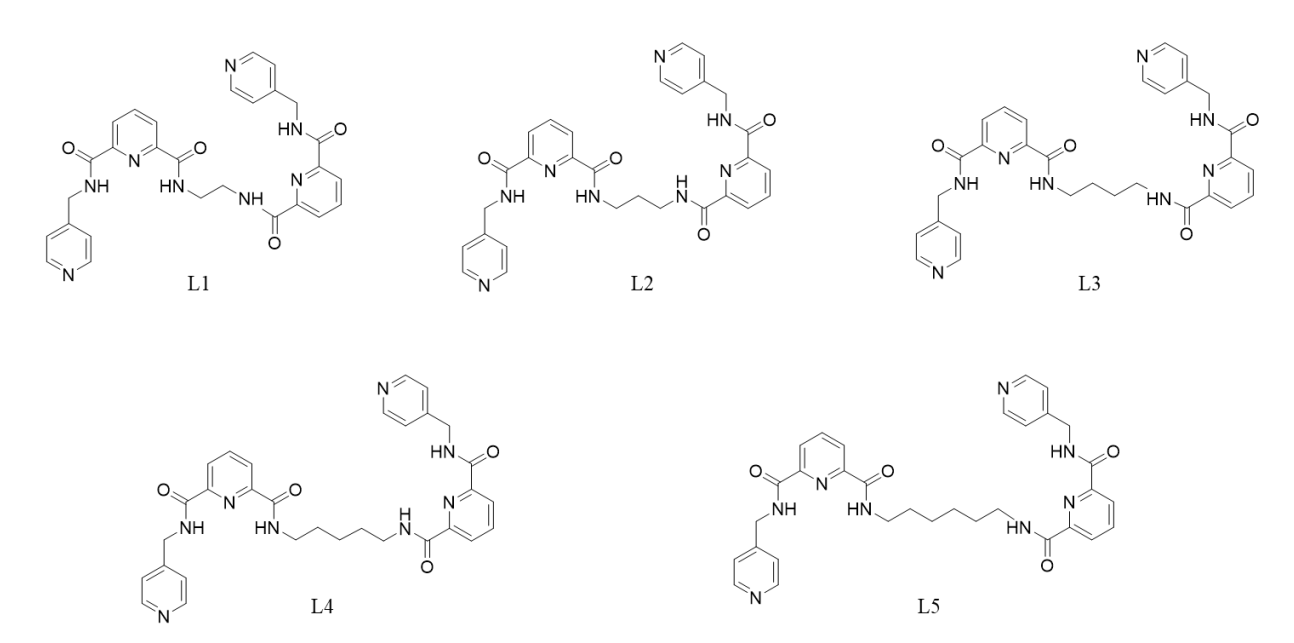


Figure 1. Structures of ligands L1–L5 designed as flexible diamide receptors with different alkyl spacers for anion binding.

Figure 2. The proposed interaction between ligand and anions (chloride, nitrate and phosphate) via hydrogen bonding interaction at NH group.

The binding interactions of these ligands with anions have been explored through UV-Vis titration studies [21-23]. To further understand the binding mechanism, ¹H NMR spectroscopic titrations were used to examine the interactions between dicarboxamide derivatives with selected anions. The ¹H NMR data enabled the verification of the NH group's involvement in hydrogen bonding by observing the distinctive downfield shift of the NH proton signals [24]. These NH groups can act as H-bond donors to interact with anions, forming a receptor—anion association complex [11]. Receptors with a greater number of hydrogen bond donors favorably bind anions with a greater number of hydrogen bond acceptors [25].

EXPERIMENTAL

Synthetic Procedures

Compounds L1 to L5 were synthesized by suspended *N*-6-[(4-pyridylmethylamino)carbonyl]-pyridine-2-carboxylic acid methyl ester with ethane-1,2-diamine, propane-1,3-diamine, butane-1,4-diamine, pentane-1,5-diamine and hexane-1,6-diamine in toluene, respectively (40 mL). The mixture was then refluxed under an inert atmosphere. After the reaction was complete, the solvent was removed under vacuum to obtain an off-white solid [22-23, 26-27].

¹H NMR Titration Methods

 1 H NMR titrations were performed by preparing stock solutions of L1 (1.88 mg, 7 mM) in DMSO- d_6 . The stock solutions of anions chloride, bromide, nitrate, phosphate, and chromate were prepared at 100 mM. Titrations were performed by adding 10 μL of the anion stock solution (100 mM) to 0.5 mL of the L1 solution contained in the NMR tube. Anions were titrated incrementally with 10 μL additions, repeated five times for a thorough analysis of each anion. These steps were repeated for L2–L5. The binding constants (K_I and K_2) were determined from the plot of the nonlinear fitting curve ΔNH_{shift}/[A-] (obtained from 1 H NMR integrals) using MATLAB software. There are two steps in the binding model for the 1:2 binding model:

$$K_I = \frac{[\text{H.G}]}{[\text{H.He}]} \tag{1}$$

$$K_2 = \frac{[\text{H.G}_2]}{[\text{H.I]H.G}]} \tag{2}$$

where the ligand is denoted by H, the anions by G, and the binding constants for the first and second steps of the binding equilibrium by K_1 and K_2 , respectively. The experimental data can be fitted using a nonlinear regression equation [28].

DFT Studies

The optimized structures of L1 – L5 with their anions (Cl⁻, Br⁻, NO₃⁻, PO₄³⁻ and CrO₄²⁻) were computed using the Density Functional Theory method. DFT studies were performed using the Gaussian 09 (G09) program package. The geometries were fully optimized without imposing constraints on the bond lengths, bond angles, or dihedral angles. The "OPT" keyword was employed to conduct geometry optimizations using the unrestricted DFT method at the B3LYP/6-311++G(d,p) level. The basis set 6-311++G(d,p) was applied to the C, H, N, and O atoms to optimize the molecular geometry at the B3LYP theoretical level.

RESULTS AND DISCUSSION

The interactions between ligands L1 to L5 and anions were investigated using ^{1}H NMR spectroscopy in deuterated dimethyl sulfoxide (DMSO- d_{6}) using the corresponding anions, such as chloride, bromide, nitrate, phosphate, and chromate salts. The analysis was performed by preparing a ligand solution with a constant concentration of 7 mM. L1 solution (0.5 mL) was placed in an NMR tube, and 10 μ L of an anion solution was titrated to the L1 solution in five increments.

The results showed that two distinct proton signals were identified for the NH groups in the ¹H NMR spectrum of L1 (Figure 3a), appearing at 9.60 ppm (H1, NH near the spacer) and 9.96 ppm (H2, NH adjacent to the pyridyl ring). When chloride anions were added to the L1 solution, these signals shifted downfield to 9.71 ppm (H1) and 10.07 ppm (H2) (Figure 3a). This downfield shift is characteristic of hydrogen bonding interactions, indicating that the

NH groups participated in hydrogen bonding with chloride ions. Such interactions cause deshielding of the NH protons, resulting in a downfield shift [24] owing to the reduced electron density around the NH groups [29]. In particular, the absence of shifted signals in the alkyl spacer and aromatic groups suggests that the interaction does not occur in these regions and is localized only to the amide moieties, as reported in the literature [30,31]. The NH of the amide group is known to donate hydrogen bonds and function as an active anion binding site. Meanwhile, for ligand L2 (Figure 3b), upon the addition of chloride anions, the NH signals exhibited a slight upfield shift, changing from 9.49 ppm (H1) and 9.82 ppm (H2) to 9.51 ppm (H1) and 9.86 ppm (H2), respectively (Figure 3b). Although hydrogen bonding usually results in a downfield shift, this unexpected upfield shift may be attributed to conformational rearrangement caused by the propyl spacer. This

spacer might adopt a geometry that weakens the NH···Cl⁻ interaction, leading to increased electron density and greater shielding around the NH protons [32]. In contrast, L1's ethyl spacer may adopt a more rigid or pre-organized conformation that enables stronger anion binding, resulting in a more pronounced downfield shift.

For L3, L4, and L5, the longer alkyl spacers provided greater flexibility, allowing effective hydrogen bonding with chloride ions. Accordingly, downfield shifts of the NH signals were observed for all three ligands, confirming the involvement of the NH groups in anion binding. Therefore, the direction and magnitude of the chemical shift changes upon chloride addition reflect the extent and strength of the NH···Cl⁻ hydrogen bonding interactions in each ligand.

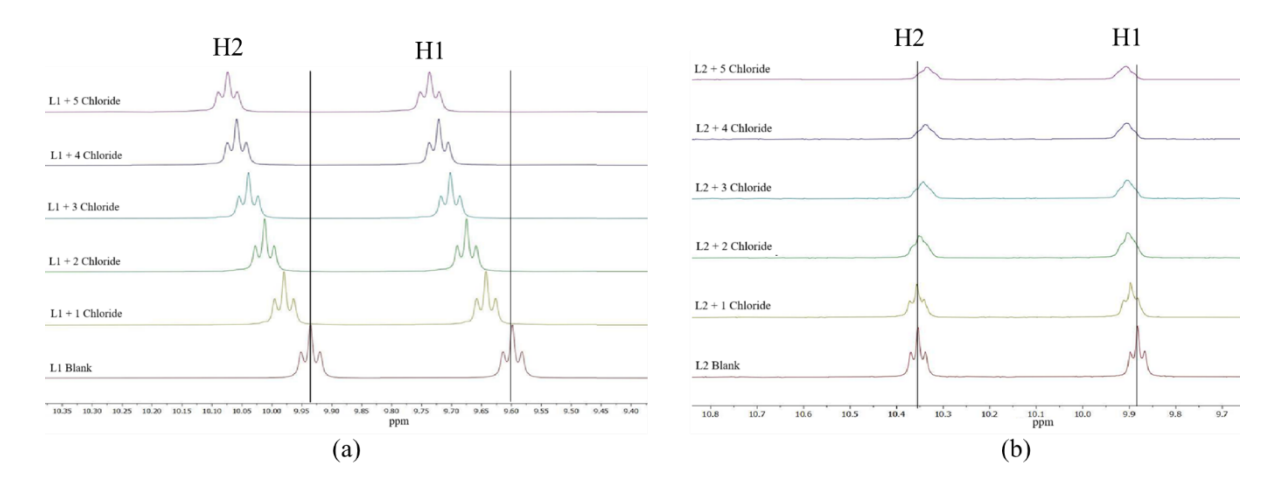


Figure 3. ¹H NMR titration of (a) L1 and (b) L2 with chloride anions in DMSO-d₆.

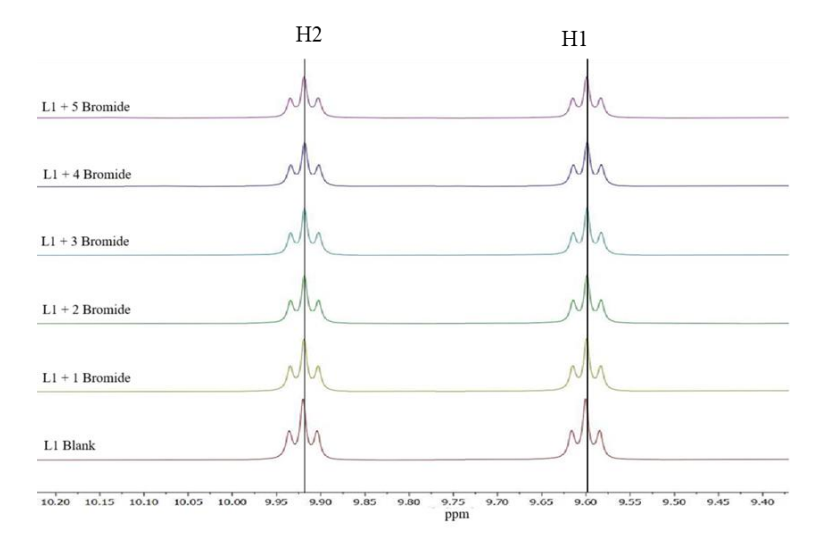


Figure 4. ¹H NMR titration of ligand L1 with bromide anions in DMSO-d₆.

Meanwhile, the addition of bromide anion to the L1 solution showed that the spectra did not change in the proton resonance (Figure 4) under identical experimental conditions when ligand L1 was titrated against chloride. This aligns with the findings reported by other researchers [33], who observed no significant chemical shift upon titration with bromide anions. A previous study [34] reported that bromide anions produce a steric effect that inhibits the formation of hydrogen bonds, which is similar to that observed for L1. This is due to the comparatively large size of

bromide compared to other halides, such as chloride, which can cause steric effects that could affect the reactivity and binding of the molecule. Ligand L2 also showed no chemical shift at the NH moieties upon titration with bromide anions, similar to L1. This trend was consistently observed throughout the investigation of ligands L2–L5. This consistency implies that the binding environment of the bromide anions is not significantly affected by the structural and electronic properties of these ligands (L1 – L5) in either the *cis* or *trans* conformations.

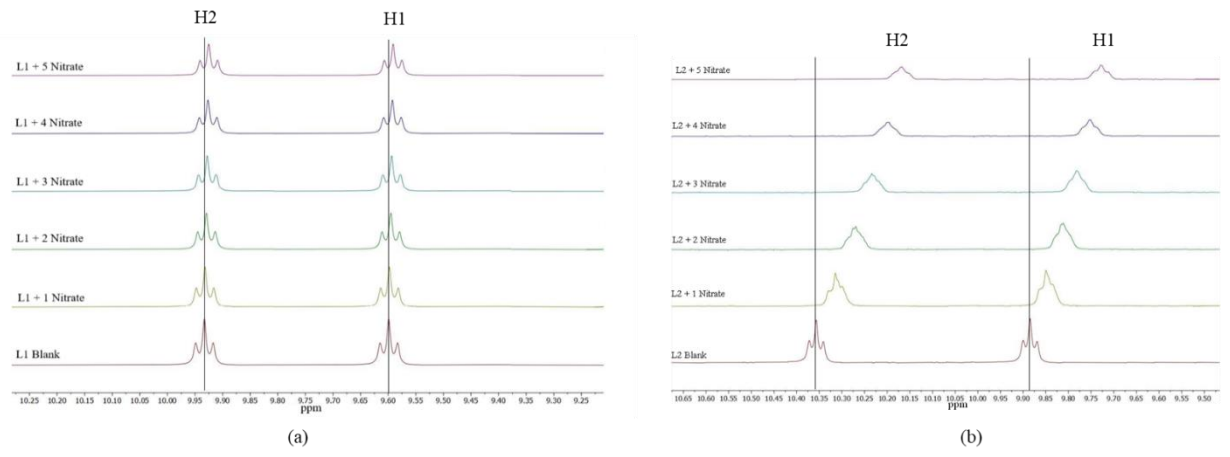


Figure 5. ¹H NMR titration of (a) L1 and (b) L2 with nitrate in DMSO-d₆.

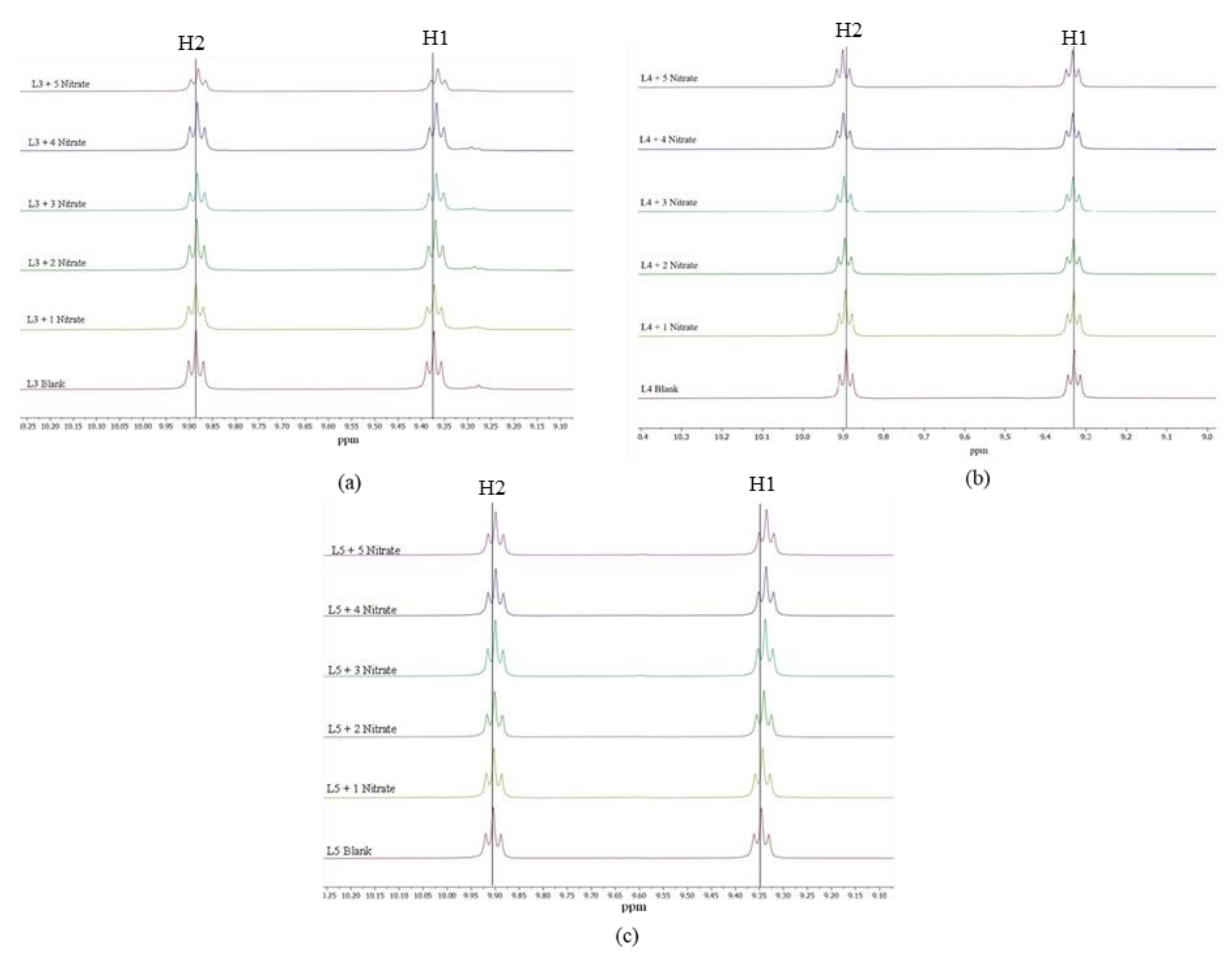


Figure 6. ¹H NMR titration of (a) L3, (b) L4 and (c) L5 with nitrate in DMSO-d₆.

The addition of nitrate anions to L1 resulted in the -NH signals at 9.60 ppm (H1) and 9.96 ppm (H2) shifting upfield to 9.59 ppm (H1) and 9.92 ppm (H2), respectively (Figure 5a). The resonance of the-NH signals induced minimal changes when nitrate anions were added, which is consistent with a previous study [35]. L2 also exhibited similar behavior, with both NH signals shifting from 9.49 ppm (H1) and 9.82 ppm (H2) to 9.32 ppm (H1) and 9.63 ppm (H2) (Figure 5b). As reported in another study [36], the upfield shifts might be attributed to the internal charge transfer that occurred between the nitrate anions (oxygen atom), amide moieties (NH groups), and aromatic (CH group).

Titration of ligands L3–L5 with nitrate showed slight shifts in the NH signals. For L3, the NH (H1) peak shifted upfield from 9.39 ppm to 9.38 ppm, whereas the NH peak (H2) remained unchanged (Figure 6a). L5 also showed upfield shifts from 9.34 ppm to 9.33 ppm (H1) and 9.90 ppm to 9.89 ppm (H2) (Figure 6c), respectively. In addition, both L3 and L5 exhibited upfield shifts in the aromatic protons of the pyridine ring (specifically at the α - and β -positions to the nitrogen atom), shifting from 8.40 to 8.60 ppm, suggesting anion- π or dipole interactions between the nitrate and pyridine moieties. Although nitrate anions are known to interact with amide NH groups, previous studies suggest that these interactions are weaker than those involving the aromatic system of the pyridine moiety [37]. This suggests that the interaction may be dominated by non-classical contacts, such as anion- π or electrostatic interactions, rather than traditional hydrogen bonding. In contrast, L4 shows a downfield shift (Figure 6b). This difference might arise from the conformational flexibility and spatial orientation imposed by the spacer length of the ligand. The odd-numbered pentyl spacer in L4 may adopt a conformation that disfavors the close proximity between the pyridine ring and the nitrate anion, reducing the π interactions. Meanwhile, the shorter (L3) and longer (L5) spacers might allow more favorable

folding or alignment of the pyridine ring toward the nitrate, facilitating the interaction.

The behavior of ligands L1 – L5 was further investigated using phosphate anions. The addition of phosphate anions to ligand L1 caused the NH peaks to shift downfield from 9.60 ppm to 9.61 ppm (H1) and from 9.96 ppm to 9.98 ppm (H2), respectively. This chemical shift indicates the formation of hydrogen bonds between the NH groups and phosphate, similar to chloride anions. However, when a high concentration of phosphate was added to L1, the NH peak at 9.61 ppm shifted to 9.57 ppm (H1), indicating an upfield shift (Figure 7a). In Figure 7b, the hydrogen peak of pyridine shifted from 8.45 ppm to 8.43 ppm, indicating hydrogen bond interactions with anions through C-H···O. The presence of C-H···O interactions is crucial for stabilizing phosphate anion encapsulation, as reported [33]. Their study found that the PO₄3- anion was stabilized inside a folded cavity by N-H···O hydrogen bonds and secondary $C-H\cdots\pi$ interactions between the 4nitrophenyl and middle phenyl rings.

For ligand L2, NH signals initially appeared at 9.49 ppm (H1) and 9.82 ppm (H2), and upon titration with phosphate anions, both shifted slightly downfield to 9.53 ppm and 9.87 ppm, respectively (Figure 8). A similar trend was observed for L3, with peaks shifting to 9.40 ppm (H1) and 9.92 ppm (H2). Ligands L4 and L5 also showed minor downfield shifts upon phosphate addition, indicating continued NH···anion interaction across the series. These consistent downfield movements suggest hydrogen bonding between the NH protons and the phosphate anions. The presence of longer spacers in L3-L5 provides greater flexibility, allowing the ligands to better accommodate the size and charge distribution of the phosphate. This adaptability may reduce steric hindrance and internal strain during binding, thereby enhancing the stability of the ligand-anion complexes.

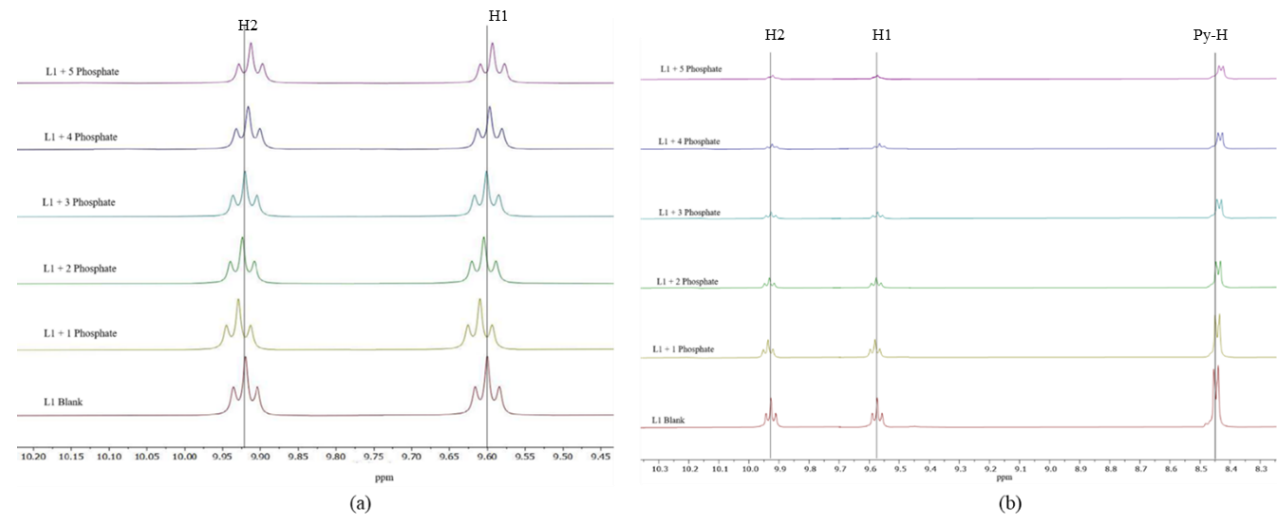


Figure 7. ¹H NMR titration of L1 (a) NH-moieties and (b) NH with pyridine (CH) moiety with phosphate in DMSO-*d*₆.

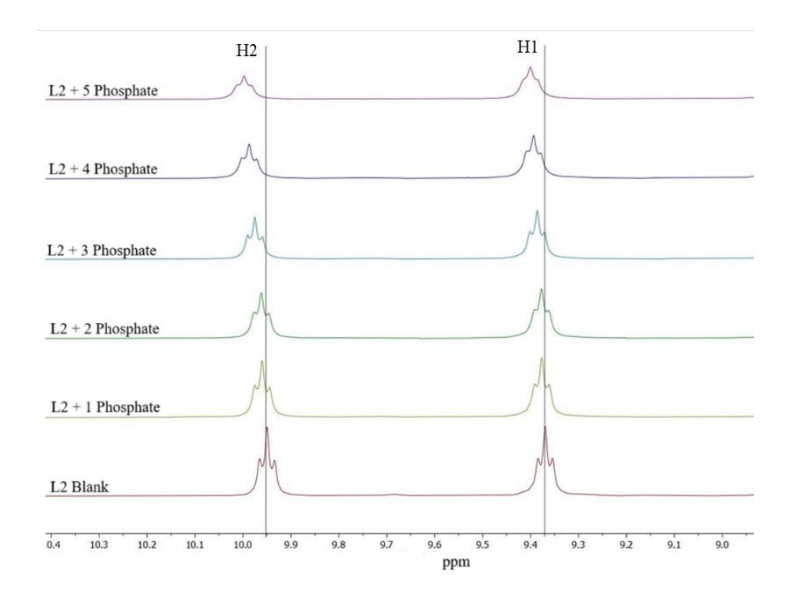


Figure 8. ¹H NMR titration of L2 with phosphate in DMSO-d₆.

The addition of chromate anions to the L1 solution resulted in the NH peaks shifting downfield to 9.62 ppm (H1) and 9.97 ppm (H2), indicating deshielding due to interactions with chromate. As more chromate was added, the -NH peaks disappeared, suggesting dynamic complex formation with multiple equilibria, possibly causing peak broadening or overlapping (Figure 9). This disappearance might be due to rapid exchange processes or the formation of higher-order complexes, as noted by [35] and [38]. The shorter ethyl spacer in ligand L1 brings the two pre-organized amides closer, enhancing the interaction between the -NH groups and chromate anions through hydrogen bonding. In contrast, ligand L2 exhibited

upfield shifts in both NH signals upon the addition of chromate, with the peaks shifting from 9.49 ppm (H1) and 9.82 ppm (H2) to 9.36 ppm and 9.66 ppm, respectively. Meanwhile, ligand L3 showed no significant changes in the NMR titration data, implying weak or no interactions with chromate anions. The longer butyl spacer in L3 may position the -NH groups too far apart for effective interaction to occur. Similarly, ligands L4 and L5, with pentyl and hexyl spacers, showed no significant changes, likely because the increased distance reduced the ability of the -NH groups to interact with chromate anions. Table 1 summarizes the titration chemical shift results obtained for L1 – L5 before and after titration with anions.

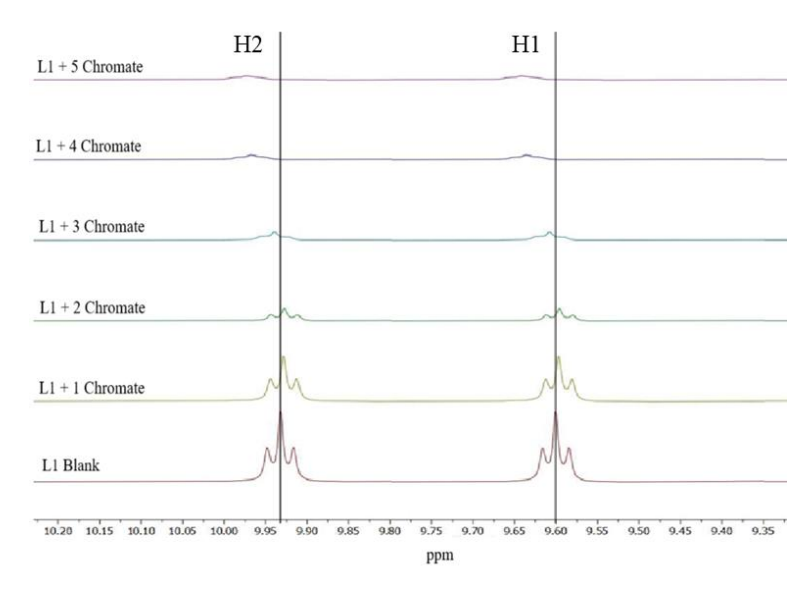


Figure 9. ¹H NMR titration of L1 with chromate in DMSO-d₆.

Table 1. The ¹ H NMR	chemical shifts of L1 -	- L5 before and after	titration with anion	s (Cl ⁻ , NO ₃ -, PO ₄ ³ -).
---------------------------------	-------------------------	-----------------------	----------------------	--

	I	L1	L	.2	L	.3	L	.4	L	.5
	NH	NH	NH	NH	NH	NH	NH	NH	NH	NH
-	9.60	9.96	9.49	9.82	9.39	9.90	9.33	9.89	9.34	9.90
Cl-	9.71	10.07	9.51	9.86	9.46	9.99	9.40	9.97	9.39	9.96
Br-	-	-	-	-	-	-	-	-	-	-
NO_3^{2-}	9.59	9.92	9.32	9.63	9.38	9.90	9.34	9.90	9.33	9.89
PO ₄ ³⁻	9.57	9.92	9.53	9.87	9.40	9.92	9.35	9.93	9.35	9.92
CrO_4^{2-}	9.62	9.97	9.36	9.66	9.38	9.89	9.34	9.90	9.33	9.89

Note: Red text indicates downfield shift, blue text indicates upfield shift, and black text indicates no significant change in chemical shift.

The shift in the -NH signals observed during the titrations was used to calculate the binding constants $(K_1 \text{ and } K_2)$, and the results are listed in Table 2. The interactions were fitted to a 1:2 (ligand:anion) binding model as expected using MATLAB software. The K_1 values for chloride ranged from 1.00 M⁻¹ to 42.08 M⁻¹. Among the ligands, L2 showed the highest K_I value (42.08 M⁻¹), consistent with the upfield shift observed for the -NH proton, suggesting strong primary binding. The K_2 values for chloride ranged from 12.46 M⁻¹ to 45.62 M⁻¹, indicating that most of the ligands in the series were capable of supporting a second chloride binding event. This may be attributed to the optimal chain length, which allows a favorable spatial arrangement of the secondary -NH donors, thereby facilitating stronger binding at the second site. Similar binding behavior has been observed in other flexible diamide-based receptors, where the spacer length controls the receptor geometry and multivalent binding [39,40]. These results indicate that chloride ions interact strongly with the hydrogen-bond donor sites (-NH) of the ligands, effectively stabilizing the primary and secondary binding sites.

Meanwhile, for bromide anions, no binding constants could be determined owing to the lack of observable physical changes in the ¹H NMR spectra. This could be attributed to the larger ionic radius and lower charge density of bromide, resulting in weaker and less directional hydrogen bonding, which limits effective binding [34].

For nitrate, the ligands displayed K_1 values in the range of 1.00 M⁻¹ to 8.26 M⁻¹, where L4 demonstrated the strongest K_1 (8.26 M⁻¹). The K_2 values for nitrate ranged from 1.00 M⁻¹ to 34.49 M⁻¹, where L2 displayed the strongest K_2 (34.49 M⁻¹), and the other ligands showed weak interactions with nitrate. These results indicate that nitrate ions bind weakly throughout the ligand series, likely owing to non-directional electrostatic or hydrogen-bonding interactions involving the amide NH protons, which possess partial positive charges and can act as hydrogen bond donors. The planar geometry and delocalized charge on the nitrate limit strong directional binding, reducing the overall interaction strength [41].

The binding constants for phosphate showed K_1 values ranging from 1.75 M⁻¹ to 22.80 M⁻¹. The strongest K_1 was observed for L1 (22.80 M⁻¹). The K_2 values were highest for L4 (21.86 M⁻¹) and L5 (17.42 M⁻¹). These results are consistent with the higher charge density and tetrahedral geometry of phosphate, which provides multiple hydrogen-bond acceptor sites that can engage in both primary and secondary binding (NH···O and CH···O) interactions. Such behavior is well documented in the recognition of oxoanions by amide-based receptors [42]. For chromate, the K_1 values ranged from 1.00 M⁻¹ to 13.82 M⁻¹. The strongest primary interaction was observed for L3 (13.82 M^{-1}), while K_2 values ranged from 1.17 M^{-1} to 36.33 M⁻¹. The relatively moderate binding affinity may be due to the larger size and lower symmetry of chromate compared to phosphate, which may reduce efficient packing and hydrogen bonding within the receptor pocket [43]. Based on the overall binding constant trends, chloride, known as a kosmotropic anion, exhibited the highest binding affinity, likely due to its strong ability to stabilize hydrogen-bonding networks [44] by showing high binding constant values compared to other anions.

Table 2. Binding constants calculated from ¹H NMR titrations for L1 – L5 in DMSO-*d*₆ for their respective anions.

	Binding Contant K values (M ⁻¹)									
	K_{I}	K_2	K_{I}	K_2	K_{I}	K_2	K_{I}	K_2	K_{I}	K_2
	Chloride		Bro	nide	Nit	rate	Phos	phate	Chro	mate
L1	1.03	45.62	-	-	1.00	1.00	22.80	3.45	1.00	36.33
L2	42.08	5.74	-	-	1.00	34.49	3.75	8.00	1.11	28.50
L3	1.06	40.72	-	-	7.68	6.11	10.97	16.09	13.82	1.17
L4	1.00	45.16	-	-	8.26	7.75	3.27	21.86	2.34	11.04
L5	4.57	12.46	-	-	4.17	15.02	1.75	17.42	7.20	12.18

DFT calculations were performed to investigate the geometric changes that occur when tetraamide ligands (L1–L5) interact with selected anions, including chloride, bromide, nitrate, phosphate, and chromate. DFT analysis revealed the most stable structures of the free ligands and their complexes, showing structural changes upon anion binding [45].

The optimized structures of L1–L5 were analyzed to understand how the spacer length affects amide flexibility and binding orientation. Significant rearrangements were observed around the NH groups, which serve as key sites for hydrogen bonding during complexation [46]. Ligands L1–L5 retained their stable trans conformations during the anion binding studies. Halide ions fit into the V-shaped cavity, whereas polyatomic anions form bidentate hydrogen bonds with NH groups through two aligned oxygen atoms.

Table 3 summarizes the DFT-optimized geometries of the ligands-anion interactions. Among the studied anions, phosphate formed the most stable complexes through NH···O and CH···O interactions, as indicated by the more negative optimization energy values. The pyridine CH proton likely participates in binding, consistent with previous findings [47]. The tetrahedral geometry and high charge density of phosphate promote

multipoint hydrogen bonding interactions. The calculated optimization energies for the phosphate complexes followed the order L5 > L4 > L3 > L2 > L1, with L5 exhibiting the most negative value (-8564259.81 kJ/mol). These trends suggest that longer alkyl spacers improve the structural adaptability and hydrogen bond formation. Previous findings reported that longer spacers enhance anion accommodation by reducing steric effects [48], whereas Rasmussen et al. highlighted improved flexibility in binding [49].

Chloride also formed stable complexes with the ligands, although with less negative optimization energies, ranging from -7197621.70 kJ/mol to -7,610,259.36 kJ/mol across the series. The chloride ion typically resides in a V-shaped cavity between the two diamide arms, engaging in up to two hydrogen bonding interactions. However, owing to its smaller ionic radius and spherical geometry, not all NH donors can interact simultaneously with chloride ions.

Nitrate complexes displayed less favorable stability, aligning with the literature findings [34], which reported limited stabilization of nitrate—anion interactions. The optimization energies ranged from –6254848.81 kJ/mol (L1) to –6667391.26 kJ/mol (L5). Although both nitrate and phosphate are oxoanions, the interaction with nitrate appears to be weaker overall.

Table 3. The calculated optimization energies for ligand-anion interactions.

Optimization Energy, kJ/mol						
	Chloride	Bromide	Nitrate	Phosphate		
L1	-7197621.70	-1828432.55	-6254848.81	-8155110.58		
L2	-7300824.54	-1839011.18	-6358086.87	-8243971.48		
L3	-7405914.18	-1849325.35	-6460944.67	-8360390.04		
L4	-7507069.18	-1859655.72	-6563794.77	-8464541.17		
L5	-7610259.36	-1869924.19	-6667391.26	-8564259.81		

Bromide complexes exhibited the weakest stability among the studied systems, which was attributed to the larger size and lower charge density of bromide compared to other anions. This finding is consistent with the experimental titration results, where bromide showed minimal interaction with the ligands. The overall complex stability is influenced by anion properties, such as size, geometry, and charge, as well as the ligand's ability to adapt structurally during coordination. Meanwhile, the chromate optimization calculations failed because of convergence issues and were thus not included in the structural comparison.

The bond length data for ligands L1–L5 with various anions, such as chloride, bromide, nitrate, and phosphate, were analyzed before and after optimization using DFT calculations. The post-optimization bond lengths support additional evidence for binding efficiency. The results presented in Table 4 provide insights into the structural changes and interaction strengths between the ligands and anions. As reported in another study, a shorter bond length implies that the hydrogen bond between the receptor and anions is much stronger [50]. The reported hydrogen bond distance for NH···O (HSO₄-) is 2.779 Å, where the N–H groups exhibit a strong attraction to the anion [50]. Before optimization, the NH···Cl

bond lengths ranged from 1.24-1.88 Å. After optimization, the bond lengths were slightly extended from 1.24 to 3.97 Å, indicating structural adjustments for the formation of hydrogen bonds. L3 showed the longest bond length (range from 2.88 to 3.05 Å). The increase in bond length suggests stabilization of the ligand-anion complex, with the optimized structure accommodating chloride ions. The NH···Br bond lengths before optimization were in the range of 1.22-1.93 Å. After optimization, the bond lengths increased slightly for all ligands, ranging from 1.64 to 3.12 Å. As can be observed, most of the NH···Br interactions were longer than the chloride interactions. This is probably due to the larger ionic radius of bromide and weaker hydrogen bonding interactions, which result in longer bond lengths, indicating weak binding compared to chloride. The NH···O bond lengths with nitrate anions were short, ranging from 0.97 to 1.42 Å before optimization and adjusted to 1.33-2.43 Å after optimization. The longer bond lengths after optimization suggest that there is an interaction, but it may have weakened the interaction slightly to allow for structural changes and reduced steric hindrance in the ligandanion complex. Phosphate interactions exhibited the greatest variability in bond lengths, ranging from 1.03 to 1.29 Å before optimization and increasing slightly to 1.47-2.12 Å after optimization.

Table 4. Bond Length (Å) Ligands-anions interaction before and after optimize with DFT studies.

	Bond Length (Å) Before Optimize								
	NH···Cl	NH···Cl	NH···Br	NH…Br	NH···O ₃ N	NH···O ₃ N	NH···O ₄ P	NH···O ₄ P	
L1	1.54, 1.73	1.43, 1.88	1.32, 2.14	1.63, 1.39	1.16, 1.16	1.13, 1.22	1.29, 1.33	1.03, 1.12	
L2	1.69, 1.48	1.72, 1.84	1.57, 1.58	1.35, 1.47	1.26, 1.06	1.13, 1.23	1.25, 1.24	1.19, 1.27	
L3	1.68, 1.46	1.61, 1.71	1.22, 1.93	1.71, 1.83	0.97, 1.03	1.26, 1.04	1.11, 1.14	1.25, 1.29	
L4	1.24, 1.56	1.38, 1.42	1.95, 1.76	1.36, 1.91	1.05, 1.19	1.04, 1.21	1.08, 1.26	1.07, 1.18	
L5	1.40, 1.56	1.24, 1.69	1.34, 1.42	1.98, 1.55	1.23, 1.29	1.18, 1.42	1.15, 1.26	1.17, 1.31	
				Bond Lengtl	h (Å) After Op	otimize			
	NH···Cl	NH···Cl	NH···Br	NH…Br	NH···O ₃ N	NH···O ₃ N	NH···O ₄ P	NH···O ₄ P	
L1	1.59, 1.72	1.70, 3.97	2.36, 3.12	1.65, 2.77	2.34, 2.77	2.28, 2.43	1.47, 2.06	1.67, 1.95	
L2	1.69, 1.48	1.72, 1.84	2.44, 2.67	2.45, 2.57	1.37, 1.32	1.94, 1.33	1.91, 1.95	1.89, 1.94	
L3	2.88, 3.04	2.89, 3.05	2.23, 2.37	2.22, 2.70	1.92, 1.96	2.07, 2.21	1.98, 2.12	1.99, 2.0	
L4	1.61, 1.63	1.59, 5.16	2.36, 2.77	2.24, 2.35	1.67, 1.88	1.80, 2.46	1.97, 2.11	1.81, 1.86	
L5	1.40, 1.56	1.24, 1.69	1.64, 2.11	2.28, 2.32	2.17, 2.02	1.93, 1.99	1.35, 1.37	2.02, 2.15	

		Binding Energies, kJ/mol							
	Chloride	Bromide	Nitrate	Phosphate					
L1	-1206184.40	-674300.76	-735164.17	-1686834.11					
L2	-1206222.53	-674548.47	-735532.35	-1697465.54					
L3	-1206406.42	-674501.71	-735537.30	-1700047.37					
L4	-1206449.37	-674555.60	-735884.80	-1700975.27					
L5	-1208290.76	-674555.61	-735892.53	-1701219.00					

Table 5. Binding energy for ligands-anions interaction.

The binding energy (ΔE) serves as an indicator of the interaction strength between ligands and anions. It was calculated using the following expression:

$$\Delta E = E_{complex} - (E_{ligand} + E_{anions})$$
 (3)

where $E_{complex}$, E_{ligand} , and E_{anion} are the optimized ground-state energies of the respective species. Table 5 summarizes the binding energies of all ligand-anion complexes.

Among all the studied anions, phosphate exhibited the strongest binding affinity for ligands L1–L5. The L5–phosphate complex exhibited the most negative binding energy (–1701219.00 kJ/mol), suggesting the most stable interaction. The increasing trend in the binding energy from L1 to L5 correlates with the spacer length, where longer alkyl chains enhance the NH···O and CH···O hydrogen bonding. This is consistent with previous studies that emphasized the role of hydrogen bonding in electrostatic stabilization [47].

The binding efficiency was assessed relative to L5-phosphate (set at 100%) using the following equation:

Binding Efficiency (%) =
$$\frac{\text{Binding Energy of Anions}}{\text{Binding Energy of L5-Phosphate}}$$

X 100% (4)

Reporting the binding energy as binding efficiency (%) allows for a direct comparison of the interaction strength across different complexes relative to the strongest binder. As shown in Table 5, the phosphate binding efficiency increased progressively from L1 (99.15%) to L5 (100%). This trend confirms that ligand flexibility and spacer length directly influence the coordination capability and interaction strength. In contrast, chloride complexes showed moderate binding energies (-1206184.40 to -1208290.76 kJ/mol) with binding efficiencies between 70.90% and 71.02%. Their lower affinity is attributed to the limited NH····Cl hydrogen bonding and the absence of significant electrostatic contributions.

Nitrate complexes displayed significantly weaker interactions, with binding energies ranging from –735164.17 to –735892.53 kJ/mol (43.21–43.26% efficiency). These interactions likely involve anion–π contacts between the nitrate and pyridine rings, which account for the moderate selectivity despite the lower overall energy [37]. Bromide complexes were the weakest binders, with energies ranging from –674300.76 to –674555.61 kJ/mol and binding efficiencies of 39.64–39.65%. Their lower affinity is consistent with the larger ionic radius and lower charge density of bromide, which reduces the hydrogen bonding capability [34].

CONCLUSION

These studies demonstrated that L1 to L5 interact with chloride anions, as evidenced by a downfield shift in the ¹H NMR peaks upon titration, except for L2, which exhibited an upfield shift. Bromide anions showed negligible interactions with all ligands, with no significant shifts observed. For the nitrate anions, L1, L2, L3, and L5 displayed upfield shifts in the NH signals, attributed to the proton-transfer process. All the ligands demonstrated hydrogen bonding interactions in the amide regions when titrated with phosphate anions. This study also suggested that chromate anions interact with ligands, with L2 showing additional C-H···O binding. Meanwhile, L3, L4, and L5 exhibited weaker interactions, as indicated by the insignificant peak shifts. The binding constant values supported the ¹H NMR findings, with chloride showing the highest affinity, followed by phosphate, chromate, and nitrate. DFT calculations, showing consistent trends with the observed chemical shifts and binding constants, further confirmed that chloride and phosphate formed the most stable complexes with the ligands, indicating strong selectivity toward these anions.

ACKNOWLEDGEMENTS

This research was supported by FRGS (vot number 59579, FRGS/1/2019/STG01/UMT/02/3) from Ministry of Education of Malaysia and we thank the Universiti Malaysia Terengganu for scientific supports.

REFERENCES

- Mujahid, A., Afzal, A. and Dickert, F. L. (2023)
 Transitioning from supramolecular chemistry to molecularly imprinted polymers in chemical sensing. *Sensors*, 23, 7457.
- Geng, W. C., Jiang, Z. T., Chen, S. L. and Guo, D. S. (2024) Supramolecular interaction in the action of drug delivery systems. *Chemical Science*, 15, 7811–7823.
- 3. Baumer, N., Matern, J. and Fernandez, G. (2021) Recent progress and future challenges in the supramolecular polymerization of metal-containing monomers. *Chemical Science*, **12**, 12248–12265.
- Kishore, R., Tripuramalu, B. K. and Das, S. K. (2015) Significant role of supramolecular interactions on conformational modulation of flexible organic cation receptors in a metalbis(dithiolate) coordination complex matrix. Crystal Growth & Design, 15, 4459–4474.
- 5. Zhao, J., Yang, D., Yang X. J. and Wu, X. (2019) Anion coordination chemistry: from recognition to supramolecular assembly. *Coordination Chemistry Reviews*, 2019, **378**, 415–444.
- Priya, E., Kumar, S., Verma, C., Sarkar, S. and Maji, P. K. (2022) A comprehensive review on technological advances of adsorption for removing nitrate and phosphate from waste water. *Journal of Water Process Engineering*, 49, 103159.
- 7. Yang, Z., Zhang, W., Liu, X., Zhao, S., Yang, Z. and Jia, X. (2023) Chloride salt of oligourea ligand: Synthesis, crystal structure, thermal analyses, and chloride anion binding properties. *Inorganic Chemistry Communication*, **151**, 110568.
- 8. Bian, Z., Wang, Y., Zhang, X., Li, T., Grundy, S., Yang, Q. and Cheng, R. (2020) A review of environment effects on nitrate accumulation in leafy vegetables grown in controlled environments. *Foods*, **9**, 732.
- Ward, M. H., Jones, R. R., Brender, J. D., Kok, T. M. D., Weyer, P. J., Nolan, C. M. Villanueva, B. T. and Breda, S. G. V. (2018) Drinking water nitrate and human health: An updated review. *International Journal Environment Research* Public Health, 15, 1557.
- 10. Yousefi, H. and Douna, B. K. (2023) Risk of nitrate residues in food products and drinking water. *Asian Pac. J. Environ. Cancer*, **6**, 69–79.

- 11. Billing, B. K. and Verma, M. (2021) Anion recognition employing -NH linked organic moieties. *Chemistry Select*, **6**, 4273–4284.
- 12. Kundu, S., Egboluche, T. K., Yousuf, Z. and Hossain, M. A. (2021) Spectroscopic and colorimetric studies for anions with a new ureabased molecular cleft. *Chemosensors*, **9**, 287.
- Chen, X., Dai, X., Xie, R., Li, J., Khayambashi, A., Xu, L., Yang, C. N., Shen, Wang, Y., He, L., Zhang, Y., Xiao, C., Chai, Z. and Wang, S. (2020) Chromate separation by selective crystallization. *Chinese Chemical Letter*, 31, 1974–1977.
- 14. Manna, U. and Das, G. (2021) An overview of anion coordination by hydroxyl, amine and amide based rigid and symmetric neutral dipodal receptors. *Coordination Chemistry Reviews*, **427**, 213547.
- 15. Kim, J., Kim, S. H., Heo, N. J., Hay, B. P. and Kim, S. K. (2023) Molecular pincers using a combination of N-H and C-H donors for anion binding. *International Journal of Molecular Science*, 24, 163.
- 16. Wang, D. X. and Wang, M. X. (2020) Exploring anion-π interactions and their applications in supramolecular chemistry. *Accounts Chemical Research*, **53**, 1364–1380.
- 17. Lopez-Martinez, L. M., Garcia-Elias, J., Ochoa-Teran, A., Ortega, H. S., Ochoa-Lara, K., Montano-Medina, C. U., Yatsimirsky, A. K., Ramirez, J. Z., Labastida-Galvan, V. and Ordonez, M. (2020) Synthesis, characterization and anion recognition studies of new fluorescent alkyl bis(naphthylureylbenzamide)-based receptors. Tetrahedron, 2017, 76, 130815.
- Vardhan, H. and Verpoort, F. (2019) UV–Vis absorption studies of coordination-driven selfassembled 2D metalla-rectangle towards multicarboxylation anions. *Polyhedron*, 157, 262–266.
- 19. Suman, K., Rajnikant, Gupta, V. K. and Sarkar, M. (2013) Cooperative effect of "flexible" interaction and "flexible" framework in reversible intake and removal of aromatic guest molecules. *Dalton Transactions*, **42**, 8492–8497.
- Kadir, M. A. and Sumby, C. J. (2018) Synthesis, Characterization and crystal structure of coordination polymers developed as anion receptor. Solid State Phenomena, 273, 134–139.
- 21. Kadir, M. A., Razak, F. I. A. and Haris, N. S. H. (2023) Anion titration studies of tetraamide compounds as a potential chromate separation

- materials. *Journal of Materials in Life Sciences*, **2**, 133–140.
- Haris, N. S. H., Shamsulazri, N. A. N., Mansor, N., Zuki, H. M., Kadir, M. A. (2022) Anion titration studies of flexible amide ligands bearing propyl spacer as potential anion receptors for dichromate. *Malaysian Journal of Chemistry*, 24, 302–310.
- 23. Kadir, M. A., Haris, N. S. H., Zuki, H. M., Kassim, S., Kassim, K. (2024) Synthesis, spectroscopic and anion titration studies of new symmetrical tetraamide molecules derived from *N*-6-[(4-pyridylmethylamino) carbonyl]-pyridine-2-carboxylic acid methyl ester. *Trends in Sciences*, 21, 7405
- Zaleskaya, M., Dobrzycki, L. and Roma'nski, J. (2020) Highly efficient, tripodal ion-pair receptors for switching selectivity between acetates and sulfates using solid-liquid and liquid-liquid extractions. *International Journal* of Molecular Sciences, 21, 9465.
- 25. Sarkar, S., Ballester, P., Spektor, M. and Kataev, E. A (2022) Micromolar affinity and higher: synthetic host–guest complexes with high stabilities. *Angewandte Chemie International Edition*, **62**, e202214705.
- Haris, N. S. H., Mansor, N., Yusof, M. S. M., Sumby, C. J. and Kadir, M. A. (2021) Investigating the potential of flexible and pre-organized tetraamide ligands to encapsulate anions in onedimensional coordination polymers: synthesis, spectroscopic studies and crystal structures. *Crystals*, 11, 77.
- 27. Kadir, M. A., Haris, N. S. H., Yusof, M. S. M., Kassim, K. and Razak, F. I. A. (2023). Dataset of spectroscopic, crystallography and DFT of novel 1,2-bis[*N*,*N*'-6-(4-pyridylmethylamido) pyridyl-2-carboxyamido]butane. *Data in Brief*, **51**, 109635.
- 28. Thordarson, P. (2011) Determining association constants from titration experiments in supramolecular chemistry. *Chemical Society Reviews*, **40**, 1305–1323.
- 29. Zarycz, M. N. C. and Guerr, C. F. (2018) NMR ¹H-Shielding constants of hydrogen-bond donor reflect manifestation of the pauli principle. *The Journal of Physical Chemistry Letter*, **9**, 3720–3724.
- 30. Ros-Lis, J. V., Manez, R. M., Sancenon, F., Soto, J., Rurack, K. and Weishoff, H. (2007) Signalling mechanisms in anion-responsive push-pull chromophores: the hydrogen-bonding,

- deprotonation and anion-exchange chemistry of functionalized azo dyes. *European Journal of Organic Chemistry*, **15**, 2449–2458.
- 31. Qin, L., Hartley, A., Turner, P., Elmes, R. B. P. and Jolliffe, K. A. (2016) Macrocyclic squaramides: anion receptors with high sulfate binding affinity and selectivity in aqueous media. *Chemical Science*, 7, 4563–4572.
- 32. Su, H., Li, J., Lin, H., and Lin, H. (2010) An efficient novel acetate anion receptor based on isatin. *Journal of Brazilian Chemical Society*, **21**, 541–545.
- 33. Wang, X., Hu, X., Song, L., Yang, X., Xiao, Q., Xu, H. and Ding, S. (2020) Efficient separation of perrhenate as analogue to pertechnetate in nitric acid solution with a DOTA-tetraamide ligand: Solvent extraction, complexation and structure study. *Journal of Molecular Structure*, 1216, 128330.
- Orenha, R. P., da Silva, V. B., Caramori, G. F., Schneider, F. S. D. S., Piotrowski, M. K., Contreras-Garcia, J., Cardenas, C., Goncalves, M. B., Mendizabal, F. and Parreira, R. L. T. (2020) On the recognition of chloride, bromide and nitrate anions by anthracene–squaramide conjugated compounds: A computational perspective. New Journal of Chemistry, 44, 17831–17839.
- 35. Khansari, M. E., Mirchi, A., Pramanik, A., Johnson, C. R., Leszczynski J. and Hossain, M. A. (2017) Remarkable hexafunctional anion receptor with operational urea-based inner cleft and thiourea-based outer cleft: Novel design with high-efficiency for sulfate binding. *Scientific Reports*, 7, 6032.
- Sahoo, H. S., Chand, D. K., Mahalakshimi, S., Mir, H. M. and Raghunathan, R. (2007) Manifestation of diamagnetic chemical shifts of proton NMR signals by an anisotropic shielding effect of nitrate anions. *Tetrahedron Lett.*, 48, 761–765.
- 37. Watt, M. M., Zakharov, L. N., Haley, M. M. and Johnson, D. W. (2013) Selective Nitrate Binding in Competitive Hydrogen Bonding Solvents: Do Anion–p Interactions Facilitate Nitrate Selectivity? *Angewandte International Edition Chemie*, **52**, 10275–10280.
- 38. Chahal, M. K., Dar, T. A. and Sankar, M. (2018) Facile synthesis of functionalized urea, imidazolium salt, azide and triazole from 2-amino-5,7-dimethyl-1,8-naphthyridine scaffold and their utilization in fluoride ion sensing. *New Journal of Chemistry*, **42**, 10059–10066.

- 39. Gale, P. A. (2010) Anion receptor chemistry: highlights from 2008 and 2009. *Chemical Society Reviews*, **39**, 3746–3771.
- 40. Custelcean, R. (2014) Anion encapsulation and dynamics in self-assembled coordination cages. *Chemical Society Reviews*, **43**, 1813–1824.
- 41. Hu, Y., Zhou, Y., Hadizadeh, M. H. and Xu, F. (2025). Unveiling the Dynamics of NO₃ at the Air–Water Interface and in Bulk Water: A Comparative Study with Cl and ClO. *Molecules*, **30**, 1724.
- 42. Sun, Z. Y., Chen, S. Q., Liang, L., Zhao, W., Yang, X. J. and Wu, B. (2023). pH-Dependent phosphate separation using a tripodal hexaurea receptor. *Chemical Communications*, **59**, 12923–12926.
- 43. Dey, S. K., Basu, A., Chutia, R., and Das, G. (2016) Anion coo dinated capsules and pseudocapsules of tripodal amide, urea and thiourea scaffolds. *RSC Advances*, 6, 26568–26589.
- 44. Nassem, B., Arif, I. and Jamal. M. A. (2021) Kosmotropic and chaotropic behavior of hydrated ions in aqueous solutions in terms of expansibility and compressibility parameters. *Arabian Journal of Chemistry*, **14**, 103405.
- 45. Mondal, D., Ahmad, M., Panwaria, P., Upadhyay, A. and Talukdar, P. (2021) Anion Recognition through Multivalent C–H Hydrogen Bonds: Anion-Induced Foldamer Formation and Transport across Phospholipid Membranes. *The Journal* of Organic Chemistry, 87, 10–17.

- Barišić, D., Lesic, F., Vlasic, M. T., Uzarevic, K., Bregovic, N. and Tomisic, V. (2022) Anion binding by receptors containing NH donating groups - What do anions prefer? *Tetrahedron*, 120, 132875.
- 47. He, X., Thompson, R. R., Clawson, S. A., Fronczek, F. R. and Lee, S. (2023) Anion receptors with nitrone C-H hydrogen bond donors. *Chemical Communications*, **59**, 4624–4627.
- 48. Liao, J., Yu, X., Chen, Q., Gao, X., Ruan, G., Shen, J. and Gao, C. (2020) Monovalent anion selective anion-exchange membranes with imidazolium salt-terminated side-chains: Investigating the effect of hydrophobic alkyl spacer length. *Journal of Membrane Science*, 599, 117818.
- 49. Rasmussen, J. K., Bothof, C. A., Atan, S. C., Fitzsimons, R. T., Griesgraber, G. W. and Hembre, J. I. (2019) Ion exchange ligand design: Improving membrane adsorber efficiencies by spacer arm manipulation. *Reactive and Functional Polymers*, **136**, 181–188.
- Deng, C. L., Bard, J. P., Lohrman, J. A., Barker, J. E., Zakharov, L. N., Johnson, D. W. and Haley, M. M. (2019) Exploiting the hydrogen bond donor/acceptor properties of PN-heterocycles: selective anion receptors for hydrogen sulfate. *Angewandte Chemie International Edition*, 58, 3934–3938.